

**To cite this article:** Xu P, Zou D L, Lü F R, et al. Nonlinear vibration characteristics of marine propulsion shafting under bending–longitudinal coupling effect[J]. Chinese Journal of Ship Research, 2019, 14(5). <http://www.ship-research.com/EN/Y2019/V14/I5/49>.

**DOI:**10.19693/j.issn.1673-3185.01389

# Nonlinear vibration characteristics of marine propulsion shafting under bending–longitudinal coupling effect



*Xu Peng<sup>1</sup>, Zou Donglin<sup>2,3</sup>, Lyu Fangrui<sup>2,3</sup>, Ta Na<sup>2,3</sup>, Rao Zhushi<sup>\*2,3</sup>*

<sup>1</sup> Naval Military Representative Office in Dalian Shipbuilding Industry Co. Ltd., Dalian 116005, China

<sup>2</sup> Institute of Vibration, Shock and Noise, Shanghai Jiao Tong University, Shanghai 200240, China

<sup>3</sup> State Key Laboratory of Mechanical System and Vibration, Shanghai Jiao Tong University, Shanghai 200240, China

**Abstract:** [Objectives] The propulsion shafting system of large ships usually has the characteristics of long shafting, large span, and small slenderness ratio. Therefore, there is often elastic coupling effect between the bending deformation and longitudinal deformation, which is easy to cause abnormal vibration of the shafting, and affect the safe and stable operation of the shafting system. In order to study the nonlinear vibration characteristics of the shaft under bending–longitudinal coupling effect, [Methods] the nonlinear vibration equations of the propulsion shafting under bending–longitudinal coupling effect were derived by using the principle of variation, and then solved by numerical methods such as finite element method (FEM) and shooting method and by approximate analysis method such as multi-scale method. Then the influence of bending–longitudinal coupling effect on the nonlinear vibration characteristics of shafting was analyzed and compared. [Results] The results show that the bending–longitudinal coupling effect causes complex vibration phenomena such as multi-frequency response, jumping phenomenon and energy transfer in the shafting response, and increases the natural frequencies in the bending and longitudinal direction of the shafting. [Conclusions] The study in this paper can provide reference for engineering design of large ship propulsion shafting.

**Key words:** propulsion shafting; bending and longitudinal coupling; FEM; shooting method; multi-scale method

**CLC number:** U664.21; U661.44

## 0 Introduction

As the core component of the marine power plant, the propulsion shafting can convert the main engine power into the propeller thrust, which is then transferred to the hull through the thrust bearing to push the ship forward. Under complex external loads such

as the excitation of propeller fluid, rotating shaft unbalance, and bearing friction, the vibration of propulsion shafting in operation will inevitably occur. Excessive vibration easily leads to fatigue and instability of the shafting, bearing wear and even failure, thus affecting the safe and stable operation of the shafting. Therefore, the vibration characteristics of ma-

**Received:** 2018 – 08 – 29

**Supported by:** Young Scientists Fund of the National Natural Science Foundation of China (11802175); China Postdoctoral Science Foundation (2018M632107)

**Authors:** Xu Peng, male, born in 1980, master, engineer. Research interest: marine engineering. E-mail: mayue@hotmail.com

Zou Donglin, male, born in 1987, Ph.D.. Research interest: ship vibration and noise reduction.

E-mail: zoudonglin.520@sjtu.edu.cn

Lyu Fangrui, female, born in 1988, Ph.D.. Research interest: design and optimization of bearing system.

E-mail: lvfangrui1107@sjtu.edu.cn

Ta Na, female, born in 1976, Ph.D., senior engineer. Research interest: research on ship vibration and noise reduction.

E-mail: wutana@sjtu.edu.cn

Rao Zhushi, male, born in 1962, Ph.D., professor. Research interest: ship vibration and noise reduction.

E-mail: zsrhao@sjtu.edu.cn

**\*Corresponding author:** Rao Zhushi

rine propulsion shafting have always been a research hotspot in this field<sup>[1-2]</sup>. The vibration of propulsion shafting includes bending vibration, torsional vibration, and longitudinal vibration. At present, the linear theory is mostly used to study the propulsion shafting, so the analysis and calculation of three kinds of vibrations can be carried out independently to simplify the model. For example, Li et al.<sup>[3]</sup> studied the bending vibration characteristics of marine propulsion shafting and focused on the analysis of the influence rule of supporting parameters on the bending vibration characteristics. Li et al.<sup>[4]</sup> studied the influence of main-engine vibration isolation on the bending vibration characteristics of propulsion shafting under ship rolling. Zhang et al.<sup>[5]</sup> studied the longitudinal vibration characteristics of marine propulsion shafting. Zhang et al.<sup>[6]</sup> analyzed the influence rule of geometrical parameters of thrust bearings on the longitudinal vibration characteristics of shafting. Hu et al.<sup>[7]</sup> studied the optimal design method for controlling the longitudinal vibration of propulsion shafting with resonance changer. Zhang et al.<sup>[8]</sup> analyzed the longitudinal vibration characteristic and vibration control strategy of propulsion shafting. Polic et al.<sup>[9]</sup> studied the torsional vibration response of shafting under the interaction between propeller and ice. Tan et al.<sup>[10]</sup> carried out simulation and experimental study on torsional vibration of large marine propulsion shafting. All the above studies are based on the linear theory. However, under the complex working conditions of real ships, these three vibration forms will produce a strong coupling effect, such as bending-torsional coupled vibration, multi-frequency, combination resonance, and self-excited vibration of the shafting. Therefore, in order to avoid the hidden dangers of engineering design, we have to establish the nonlinear dynamic model of propulsion shafting.

The coupling nonlinear vibration of marine propulsion shafting in different directions has been studied. For example, Hua et al.<sup>[11]</sup>, Hua<sup>[12]</sup>, and Zhang et al.<sup>[13]</sup> analyzed the bending-torsional coupled vibration of the propulsion shafting under the friction excitation of water-lubricated rubber bearings and the conditions of self-excited vibration caused by bearing friction. Liu et al.<sup>[14]</sup> studied the bending-torsional coupled vibration of the shafting caused by the eccentricity of the propeller and analyzed the fatigue stress of the shafting. Zhu et al.<sup>[15]</sup> studied the bending-torsional coupled vibration of shafting under the coupling impact of lubrication. Jiang et al.<sup>[16]</sup> studied the

bending-longitudinal coupled vibration of propulsion shafting caused by friction excitation. In recent years, research results in this field have emerged in endlessly, indicating that the influence of the nonlinear effect of shafting on its vibration characteristics has attracted attention in the industry.

In the above studies, the nonlinear effects are caused by the existence of nonlinear excitation sources (such as friction excitation). However, in practical engineering applications, large geometric deformation will also cause the nonlinear effects of shafting. For the propulsion shafting of small ships, the stiffness is large, and the geometric nonlinear effect is small. However, the propulsion shafting of large ships is generally very long (possibly hundreds of meters in span), and the slenderness ratio is small (the slenderness ratio is the ratio of the turning radius of shafting section to the shafting length; the smaller slenderness ratio can lead to the more "flexible" shafting, which is an important index to investigate the beam stiffness in engineering). Under the excitation of propeller fluid and unbalanced load, the large transverse deformation of shafting is easy to occur, and then there is serious elastic coupling between longitudinal deformation and transverse deformation. This is the beam bending – longitudinal coupled vibration caused by the geometric nonlinearity of large deformation. Based on this, this paper intends to establish and solve the bending-longitudinal coupled nonlinear dynamic equation of the marine propulsion shafting. Then it uses the finite element method (FEM) and multi – scale method to analyze the abnormal vibration of propulsion shafting when the bending-longitudinal coupled nonlinear effect occurs, so as to provide a reference for the engineering design of large marine propulsion shafting.

## 1 Bending – longitudinal coupled nonlinear dynamic model of marine shafting

Typical marine propulsion shafting consists of propeller, back stern bearing, front stern bearing, intermediate bearing, and thrust bearing, as shown in Fig. 1. In this paper, it is assumed that the shafting has uniform section, and the propeller is simplified to lumped mass. Moreover, each bearing is simplified to spring and damping.

Based on Rayleigh mechanical model of beams and Hamilton variation principle, a partial differential equation for the vibration of propulsion shafting

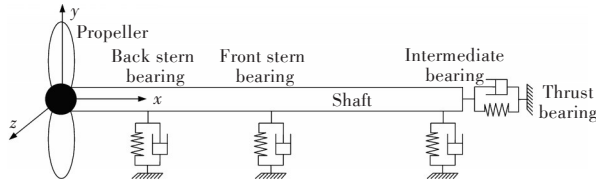


Fig.1 Schematic of marine propulsion shafting

considering the bending–longitudinal coupled nonlinear effect is established <sup>[17]</sup>:

$$\begin{aligned} \rho A \ddot{u} - EA u'' - \frac{1}{2} EA (v'^2 + w'^2)' &= 0 \\ \rho A \ddot{v} + EI_d v'''' - \rho I_d v'' + \sum_{j=1}^3 k_j v \delta(x - x_j) - EA(u'v)' - \\ &\frac{1}{2} EA(w'^2 v' + v'^3)' = 0 \\ \rho A \ddot{w} + EI_d w'''' - \rho I_d w'' + \sum_{j=1}^3 k_j w \delta(x - x_j) - EA(u'w)' - \\ &\frac{1}{2} EA(v'^2 w' + w'^3)' = 0 \end{aligned} \quad (1)$$

where  $\rho$  is the density of shaft section;  $A$  is the cross-sectional area of shaft section;  $u$ ,  $v$ ,  $w$  are the longitudinal ( $x$ -direction), transverse ( $y$ -direction), and vertical ( $z$ -direction) vibration displacements of shafting respectively;  $E$  is the elastic modulus;  $I_d$  is the second moment of area;  $k_j$  is the stiffness of each radial bearing,  $j = 1, 2, 3$ ;  $x$  is the longitudinal distance of shafting;  $x_j$  is the longitudinal distance between the propeller and each radial bearing;  $\delta(x)$  is the Dirac function.

Equation (1) lists the nonlinear terms caused by bending–longitudinal coupling. The physical meaning of the last term of the first equation is the additional force generated in the longitudinal direction when the shafting undergoes bending deformation. The physical meaning of the penultimate term of the second and third equations is the additional force generated in the bending direction when the shafting undergoes longitudinal deformation. The physical meaning of the last term of the second and third equations is the additional force generated by the inter-coupling of transverse and vertical deformation when the shafting has a large bending deformation. If these nonlinear terms are ignored, Equation (1) can be simplified to the partial differential equation for the linear vibration of shafting.

In Equation (1), the force balance boundary conditions to be met at both ends of the shafting are as follows:

$$\left\{ \begin{aligned} EA u' \Big|_{x=0}^{x=L} + \frac{1}{2} EA w'^2 \Big|_{x=0}^{x=L} + \frac{1}{2} EA v'^2 \Big|_{x=0}^{x=L} + M_1 \ddot{u} \Big|_{x=0} + \\ k_t u \Big|_{x=L} - F \cos(\omega t + \alpha) \Big|_{x=0} &= 0 \\ -\rho I_d \ddot{v}' \Big|_{x=0}^{x=L} - \Omega \rho I_p \dot{w}' \Big|_{x=0}^{x=L} + EI_d v'' \Big|_{x=0}^{x=L} - M_1 \ddot{v} \Big|_{x=0} - \\ EA u' v' \Big|_{x=0}^{x=L} &= 0 \\ EI_d v'' \Big|_{x=0}^{x=L} + J_{d1} \dot{v}' \Big|_{x=0}^{x=L} + \Omega J_{p1} \dot{w}' \Big|_{x=0}^{x=L} &= 0 \\ -\rho I_d \ddot{w}' \Big|_{x=0}^{x=L} + \Omega \rho I_p \dot{v}' \Big|_{x=0}^{x=L} + EI_d w'' \Big|_{x=0}^{x=L} - M_1 \ddot{w} \Big|_{x=0} - \\ EA u' w' \Big|_{x=0}^{x=L} &= 0 \\ EI_d w'' \Big|_{x=0}^{x=L} + J_{d1} \dot{w}' \Big|_{x=0}^{x=L} - \Omega J_{p1} \dot{v}' \Big|_{x=0}^{x=L} &= 0 \end{aligned} \right. \quad (2)$$

where  $L$  is shafting length;  $M_1$  is the propeller mass;  $k_t$  is the stiffness of thrust bearing;  $F$  is external excitation load;  $t$  is time;  $\alpha$  is load phase;  $\Omega$  is the rotation speed of shaft;  $\omega = 7\Omega$ , is the rotation speed under the secondary excitation frequency of blade (7-blade propeller);  $I_p$  is the polar moment of inertia of shaft;  $J_{d1}$  is the radial rotational inertia of propeller;  $J_{p1}$  is the polar rotational inertia of propeller.

In Equation (2), the first equation indicates the longitudinal force equilibrium, the second and third equations the transverse shear equilibrium and the moment equilibrium, respectively, and the fourth and fifth equations the vertical shear equilibrium and moment equilibrium respectively. Similarly, if nonlinear terms are ignored, Equation (2) can be simplified to the force balance boundary conditions required by the partial differential equation of the linear vibration of shafting.

## 2 Solving method of nonlinear equation

The definite solution problem of the partial differential equations shown in Equation (1) and Equation (2) can be solved by FEM <sup>[18–19]</sup> or by approximate analytical method such as multi-scale method after further dimension reduction <sup>[17]</sup>. The FEM has a simple solving process and is applicable to the shafting with arbitrary geometry, which has certain generality. However, this method is a numerical method, and it is difficult to obtain the analytical solution to the system, so it cannot reveal some mechanisms. The multi-scale method is an asymptotic analytical method, so the analytical solution to the nonlinear system can be obtained, but its solving process is complicated. In this paper, both the two methods will be used for solution. In Sections 3.1–3.3, FEM is used to analyze the vibration when the system produces the bend-

ing-longitudinal coupling effect. In Section 3.4, the multi-scale method is used to analyze the influence rule of the related parameters of shafting on the bending-longitudinal coupling effect of the system.

## 2.1 Finite element method

After the finite element theory is applied to Equation (1) and Equation (2), the element mass matrix  $\mathbf{M}^e$ , gyroscopic matrix  $\mathbf{G}^e$ , and element stiffness matrix  $\mathbf{K}^e$  can be deduced, where  $\mathbf{K}^e$  contains  $\mathbf{K}_1^e$  (linear stiffness matrix),  $\mathbf{K}_2^e$  (first displacement stiffness matrix), and  $\mathbf{K}_3^e$  (second displacement stiffness matrix). The composition of  $\mathbf{M}^e$ ,  $\mathbf{G}^e$ , and  $\mathbf{K}_1^e$  is completely consistent with the linear situation, so no specific form is listed here, and only the nonlinear stiffness matrices  $\mathbf{K}_2^e$  and  $\mathbf{K}_3^e$  are listed.

$$\mathbf{K}_2^e = \frac{EA}{2L} \begin{bmatrix} 0 & a & b & c & d & 0 & -a & e & -c & f \\ a & 0 & 0 & 0 & 0 & -a & 0 & 0 & 0 & 0 \\ b & 0 & 0 & 0 & 0 & -b & 0 & 0 & 0 & 0 \\ c & 0 & 0 & 0 & 0 & -c & 0 & 0 & 0 & 0 \\ d & 0 & 0 & 0 & 0 & -d & 0 & 0 & 0 & 0 \\ 0 & -a & -b & -c & -d & 0 & a & -e & c & -f \\ -a & 0 & 0 & 0 & 0 & a & 0 & 0 & 0 & 0 \\ e & 0 & 0 & 0 & 0 & -e & 0 & 0 & 0 & 0 \\ -c & 0 & 0 & 0 & 0 & c & 0 & 0 & 0 & 0 \\ f & 0 & 0 & 0 & 0 & -f & 0 & 0 & 0 & 0 \end{bmatrix} \quad (3)$$

$$\mathbf{K}_3^e = \frac{EA}{4L} \begin{bmatrix} 0 & 0 & 0 & 0 & 0 & 0 & 0 & 0 & 0 & 0 \\ 0 & \bar{a} & \bar{b} & 0 & 0 & 0 & -\bar{a} & \bar{c} & 0 & 0 \\ 0 & \bar{b} & \bar{d} & 0 & 0 & 0 & -\bar{b} & \bar{e} & 0 & 0 \\ 0 & 0 & 0 & \bar{f} & \bar{g} & 0 & 0 & 0 & -\bar{f} & \bar{h} \\ 0 & 0 & 0 & \bar{g} & \bar{i} & 0 & 0 & 0 & -\bar{g} & \bar{j} \\ 0 & 0 & 0 & 0 & 0 & 0 & 0 & 0 & 0 & 0 \\ 0 & -\bar{a} & -\bar{b} & 0 & 0 & 0 & \bar{a} & -\bar{c} & 0 & 0 \\ 0 & \bar{c} & \bar{e} & 0 & 0 & 0 & -\bar{c} & \bar{k} & 0 & 0 \\ 0 & 0 & 0 & -\bar{f} & -\bar{g} & 0 & 0 & 0 & \bar{f} & \bar{l} \\ 0 & 0 & 0 & \bar{h} & \bar{j} & 0 & 0 & 0 & \bar{l} & \bar{m} \end{bmatrix} \quad (4)$$

where the coefficients such as  $a \sim f$  and  $\bar{a} \sim \bar{m}$  are shown in Reference [19].

After  $\mathbf{M}^e$ ,  $\mathbf{G}^e$ , and  $\mathbf{K}^e$  of each shafting unit are assembled together and the influence of lumped mass, support spring, and damping is considered, the vibration differential equation of the shafting under the bending - longitudinal coupling effect can be obtained:

$$\mathbf{M}\ddot{\mathbf{q}}(t) + \bar{\mathbf{C}}\dot{\mathbf{q}}(t) + \mathbf{K}\mathbf{q}(t) = \mathbf{F}(t) \quad (5)$$

where  $\mathbf{q}(t)$  is the displacement vector;  $\bar{\mathbf{C}} = \Omega\mathbf{G} + \mathbf{C}$ , where  $\mathbf{C}$  is the damping matrix;  $\mathbf{F}(t)$  is the load vector.

Numerical integration methods such as Newmark method can be used to solve Equation (5). When the nonlinearity of the system is weak, a high accuracy

of the solution can be obtained by reducing the step size. However, if the system is highly nonlinear, even if the step size is small and the calculation amount is large, the accuracy of the solution is not satisfactory. At this time, the Newton-Raphson method can be used for solution. First, the approximate solution at the time step is obtained by the Newmark method, and then the Newton-Raphson method is used for further searching to obtain the more accurate numerical solution<sup>[18]</sup>. If the periodic solution to the system is needed, the shooting method can also be combined, as shown in Reference [19].

## 2.2 Multi-scale method

It is assumed that  $x^* = \frac{x}{L}$ ,  $t^* = \frac{ar}{L^2} \sqrt{\frac{E}{\rho}} t$ ,  $u^* = \frac{u}{e_0}$ ,  $v^* = \frac{v}{e_0}$ ,  $w^* = \frac{w}{e_0}$ ,  $\Omega^* = \frac{L^2}{ar} \sqrt{\frac{\rho}{E}} \Omega$ , where  $a$  is a constant;  $r = \sqrt{I_d/A}$  is the turning radius of the section;  $e_0$  is the approximate eccentricity of lumped mass. For simplicity of expression, the asterisks in the dimensionless variables  $x^*$ ,  $t^*$ ,  $u^*$ ,  $v^*$ ,  $w^*$  and  $\Omega^*$  are removed and then substituted into Equation (1). There are

$$\begin{aligned} a^2 s^2 \ddot{u} - u'' - \frac{1}{2} \frac{e_0}{L} (v'^2 + w'^2)' &= 0 \\ a^2 s^2 \ddot{v} + s^2 v''' - \frac{e_0}{L} (u' v)' - a^2 s^4 \ddot{v}'' - \\ 2\Omega a^2 s^4 \dot{w}'' + \sum_{j=1}^3 K_j v &= 0 \\ a^2 s^2 \ddot{w} + s^2 w''' - \frac{e_0}{L} (u' w)' - a^2 s^4 \ddot{w}'' + \\ 2\Omega a^2 s^4 \dot{v}'' + \sum_{j=1}^3 K_j w &= 0 \end{aligned} \quad (6)$$

where  $s = \sqrt{\frac{I_d}{AL^2}}$  is the slenderness ratio;  $K_j$  is the stiffness ratio (the ratio of bearing stiffness to longitudinal stiffness of the shafting) and  $\int_0^1 K_j dx = \frac{k_j L}{EA}$ .

The partial differential equation shown in Equation (6) can be transformed into ordinary differential equation by the Galerkin method, and the trial function will adopt a linear modal shape. It is assumed that  $u(x, t) = \phi_1(x)X_1(t)$ ,  $v(x, t) = \phi_1(x)Y_1(t)$ , and  $w(x, t) = \psi_1(x)Z_1(t)$ , where  $\phi_1(x)$  is the longitudinal first-order modal shape;  $\phi_1(x)$  is the first-order modal shape of transverse bending;  $\psi_1(x)$  is the first-order modal shape of vertical bending;  $X_1(t)$ ,  $Y_1(t)$ , and  $Z_1(t)$  are the longitudinal, transverse, and vertical vibration displacements on time scales re-

spectively. After the above is substituted into Equation (6), based on the boundary conditions and modal damping, there is

$$\begin{aligned} \ddot{X}_1 + 2\xi_u \omega_u \dot{X}_1 + \omega_u^2 X_1 &= F_1 \cos(\omega_1 t + \alpha) + \varepsilon \gamma_1 (Y_1^2 + Z_1^2) \\ \ddot{Y}_1 + 2\xi_v \dot{Y}_1 + Y_1 + \beta \dot{Z}_1 &= \varepsilon \gamma_2 X_1 Y_1 \\ \ddot{Z}_1 + 2\xi_v \dot{Z}_1 + Z_1 - \beta \dot{Y}_1 &= \varepsilon \gamma_2 X_1 Z_1 \end{aligned} \quad (7)$$

where  $\xi_u$  and  $\xi_v$  are the longitudinal and transverse modal damping ratios, respectively;  $\omega_u$  is the first-order dimensionless longitudinal natural frequency,  $F_1 = \frac{FL\phi_1(0)}{EAe_0}$ ;  $\omega_1$  is the dimensionless blade frequency speed, and for a 7-blade propeller,  $\omega_1 = 7\Omega^*$ ;  $\varepsilon$ ,  $\gamma_1$ , and  $\gamma_2$  are calculation coefficients, and  $\varepsilon \gamma_1 = -\frac{e_0}{2L} \int_0^1 \phi_1' \phi_1'^2 dx = -\frac{e_0}{2L} \int_0^1 \phi_1' \psi_1'^2 dx$ ,

$$\varepsilon \gamma_2 = -\frac{e_0}{L} \int_0^1 \phi_1' \phi_1'^2 dx = -\frac{e_0}{L} \int_0^1 \phi_1' \psi_1'^2 dx; \beta = 2\Omega \alpha^2 s^4 \left( \frac{J_{d1} \psi_1'(0) \phi_1'(0)}{\rho I_d L} + \int_0^1 \phi_1' \psi_1' dx \right).$$

Equation (7) is obtained based on the variation principle and the Galerkin method. In fact, for the energy functional, Equation (7) can also be obtained by the Ritz method combined with Lagrange equation, as shown in Reference [20]. With the multi-scale method and the classical Runge–Kutta method [21] to solve Equation (7), the nonlinear vibration characteristics of the shafting under bending–longitudinal coupling can be obtained.

### 3 Influence of bending – longitudinal coupling effect on vibration characteristics of shafting

This section will explain the influence of bending–longitudinal coupling effect on the nonlinear vibration characteristics of shafting, such as multi-frequency, jumping and energy migration. It will briefly analyze the influence of various parameters of shafting (such as support bearing, propeller mass, and slenderness ratio of shafting) on the nonlinear strength of bending–longitudinal coupling.

#### 3.1 Multi-frequency response

For linear systems, the frequency component of the steady-state response is always consistent with the excitation force. However, for nonlinear systems, in addition to the frequency component of the excitation force, other frequency components may appear in the response, namely the multi-frequency response. With the propulsion shafting shown in Table 1

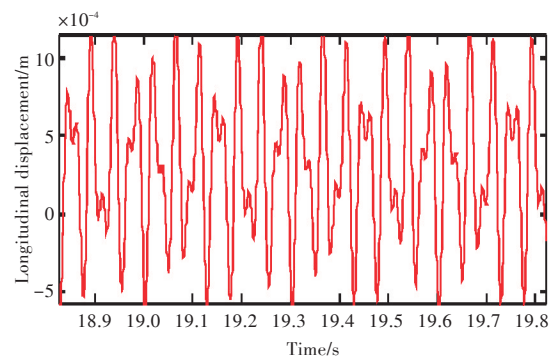
as the research object, the FEM introduced above is used for solution.

**Table 1 The main parameters of propulsion shafting**

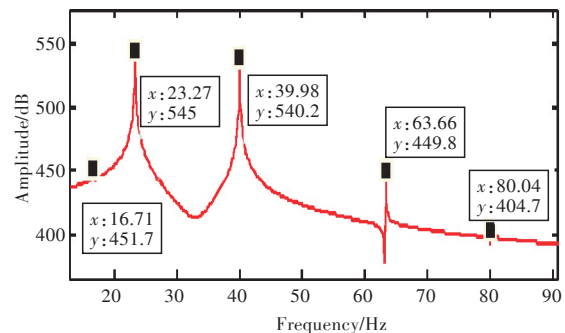
Parameter	Value/attribute
Shaft length/m	14.46
Outer diameter/mm	280
Inner diameter/mm	165
Material	Q235
Proeller mass /kg	1 300
Stiffness of thrust bearing /( $\text{N} \cdot \text{m}^{-1}$ )	$1.34 \times 10^{10}$
Damping coefficient of thrust bearing	0.01
Stiffness of intermediate bearing/( $\text{N} \cdot \text{m}^{-1}$ )	$3.05 \times 10^8$
Damping coefficient of stern bearing	0.01
Stiffness of intermediate bearing/( $\text{N} \cdot \text{m}^{-1}$ )	$1.06 \times 10^8$
Damping coefficient of intermediate bearing	0.01

It is assumed that the excitation frequency  $f_{\text{longitudinal}}$  of longitudinal blades of the shafting is 23.3 Hz, and the excitation frequency  $f_{\text{transverse}}$  of transverse blades is 20 Hz. The vibration response of shafting is calculated by the Newmark method and Newton–Raphson method. The time domain and frequency domain of the response at the midpoint of shafting are selected as the study objects. The calculation results are shown in Fig. 2.

Fig. 2 shows that although both transverse and longitudinal excitations are single-frequency excitations, other new frequency components appear in the response in addition to the excitation frequency component after considering the bending–longitudinal nonlinear coupling effect (Table 2).

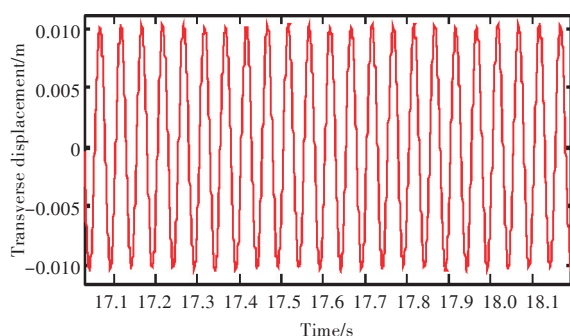
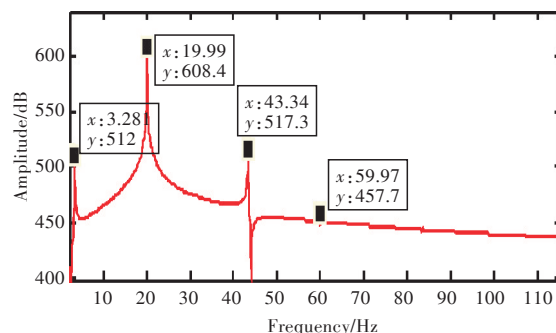


(a) Time-history curve of longitudinal displacement at  $L/2$



(b) Frequency spectrum of longitudinal displacement at  $L/2$



(c) Time-history curve of transverse displacement at  $L/2$ (d) Frequency spectrum of transverse displacement at  $L/2$ Fig.2 Time domain and frequency domain response at  $L/2$  of shafting

It can be seen that even if there is only single frequency excitation, the bending-longitudinal nonlinear coupling effect of shafting will lead to multi-frequency response. The new frequency components are various combinations of excitation frequencies, and the combination forms are mainly related to the nonlinear order and response product. Equation (1) shows that the nonlinear order of the bending-longitudinal coupling of shafting is mainly quadratic and cubic, and the product of bending response and longitudinal response is dominant. Therefore, the new frequency component is also represented as two or three times of the excitation frequency. Moreover, the product relationship in the response is reflected as the addition and subtraction of excitation frequency in the spectrum.

The team of authors has tested the vibration response of the propulsion shafting of several ships in service. According to the test results, the above multi-frequency response is real.

Table 2 The new frequency components in the response

Displacement direction	Frequency component
Transverse	$ f_{\text{transverse}} - f_{\text{longitudinal}}  = 3.3 \text{ Hz}$ , $f_{\text{transverse}} + f_{\text{longitudinal}} = 43.3 \text{ Hz}$ , $3f_{\text{transverse}} = 60 \text{ Hz}$
Longitudinal	$ 2f_{\text{transverse}} - f_{\text{longitudinal}}  = 16.7 \text{ Hz}$ , $ 2f_{\text{transverse}} + f_{\text{longitudinal}}  = 63.3 \text{ Hz}$ , $2f_{\text{transverse}} = 40 \text{ Hz}$ , $4f_{\text{transverse}} = 80 \text{ Hz}$

### 3.2 Jumping response

In this section, the FEM and shooting method are combined for solution<sup>[19]</sup>. The amplitude - frequency response curves of shafting under blade frequency excitation are shown in Fig. 3 when the shafting is accelerated or decelerated. The figure shows as follows: 1) The bending-longitudinal coupling effect shows a "hard spring" characteristic, so the resonance frequency of shafting is slightly higher than the linear natural frequency. 2) At some frequency points, the

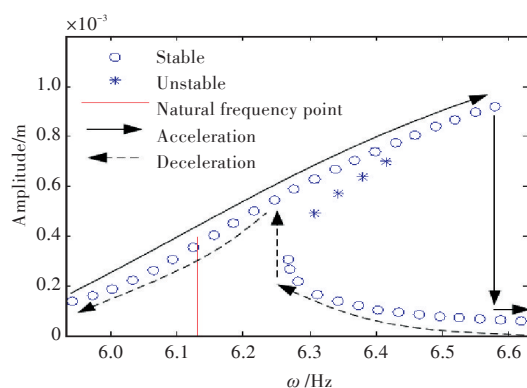


Fig.3 Amplitude frequency response curves of shaft under blade frequency excitation

response curve has three solutions at the same time (two stable solutions and one unstable solution), so there is jumping.

From a physical point of view, the bending-longitudinal nonlinear coupling effect will cause positive nonlinear stiffness of the shafting. This will be superimposed on the original linear stiffness, thus increasing the resonance frequency of the shafting.

Fig. 4 shows the amplitude-frequency response curves of shafting with different damping ratios and slenderness ratios (in the figure,  $\sigma$  is the frequency detuning parameter, and  $7\Omega - \varepsilon^2\sigma = w_f$  where  $w_f$  is the first-order transverse forward natural frequency of shafting). As can be seen from Fig. 4, the smaller damping ratio and slenderness ratio can lead to the stronger nonlinear effect of the bending-longitudinal coupling of the shafting. Therefore, the geometric nonlinear effect can be suppressed by enlarging the damping ratio, thereby improving the stability of the shafting.

### 3.3 Energy migration

It is well known that for linear vibration, the vibra-

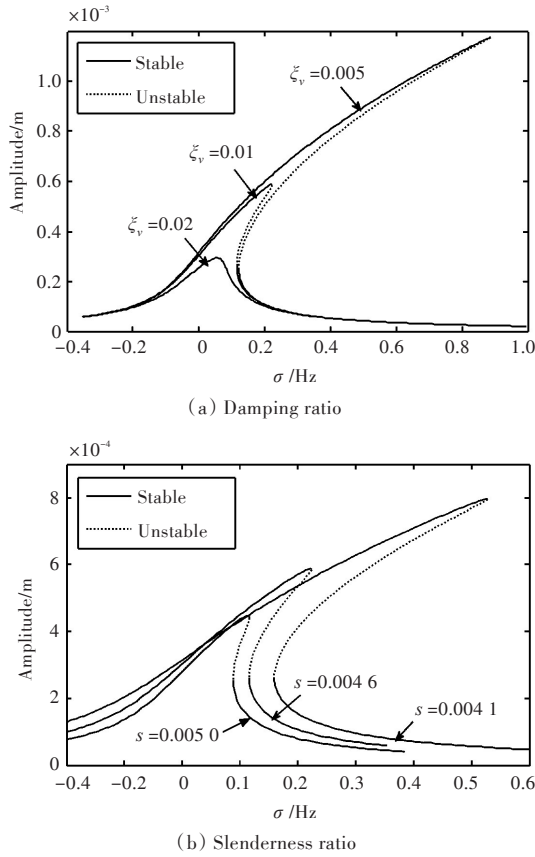


Fig.4 Variation of amplitude frequency response curves with damping ratio and slenderness ratio

tion in all directions is independent of each other and does not interfere with each other. However for nonlinear vibration, there may be energy migration between vibrations in all directions. As shown in Fig. 5, when the bending–longitudinal coupling effect exists in the shafting, there is energy penetration between bending vibration and longitudinal vibration under certain working conditions. In Fig. 5,  $a_u$  is the longitudinal vibration amplitude;  $a_v$  is the forward amplitude of bending vibration;  $b_v$  is the backward amplitude of bending vibration. In the calculation process, the excitation force is applied only in the longitudinal direction, and there is no load in the bending direction<sup>[20,22]</sup>. It can be seen from the figure that for the critical load  $f_2$ , when the excitation force is less than  $f_2$ , the longitudinal vibration amplitude increases linearly with the rise of excitation force, and the bending vibration amplitude is 0, which is consistent with the conclusion of linear vibration. When the excitation force is greater than  $f_2$ , the longitudinal vibration amplitude will remain unchanged with the further increase in excitation force. After the energy is saturated, the excess energy will be transferred to the bending direction, which will further increase the bending vibration amplitude. Meanwhile,

the forward and backward energy distribution is inversely proportional to the precession frequency<sup>[22]</sup>, so backward amplitude is higher than forward amplitude.

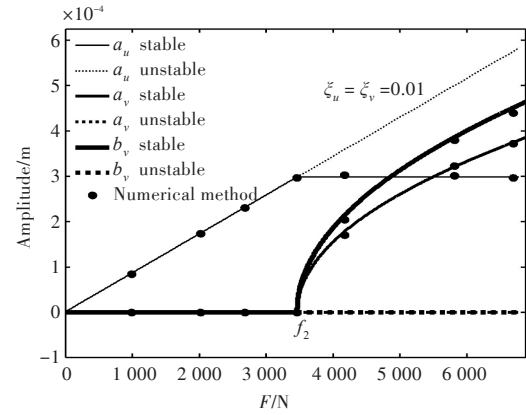


Fig.5 Variation of longitudinal vibration amplitude and bending vibration amplitude with excitation force

The critical load  $f_2$  is closely related to the system parameter, excitation frequency, and nonlinear strength. Fig. 6 shows the variation of critical load  $f_2$  with the damping ratio of system. It can be seen from the figure that as the damping ratio decreases, the critical load  $f_2$  also reduces, indicating that energy migration can also occur under small excitation force.

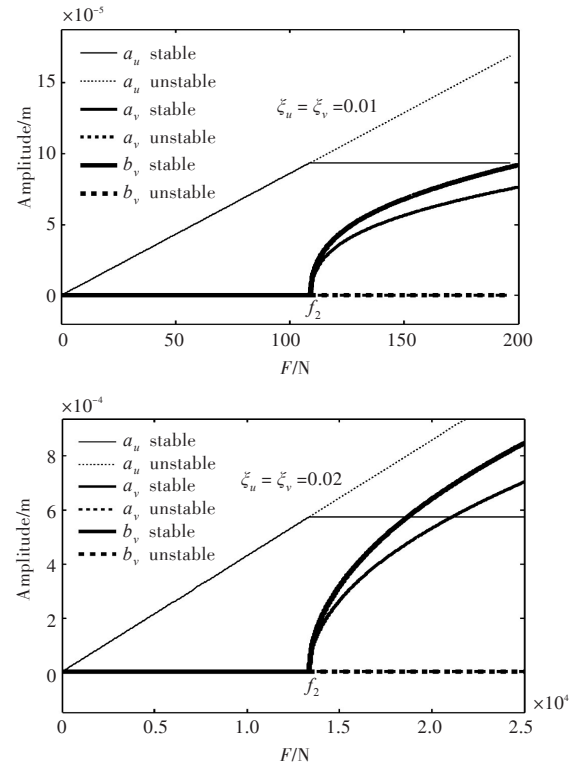


Fig.6 Variation of critical load with damping ratio

In the design of propulsion shafting, in order to effectively control the longitudinal vibration of the shafting, the characteristic of energy penetration can be fully used to keep the longitudinal vibration am-

plitude at a "limit value" without increasing further with the rise of the longitudinal excitation force.

### 3.4 Influence of shafting parameters on nonlinear strength of system

In this section, the influence of parameters such as bearing stiffness, propeller mass, and slenderness ratio on the nonlinear parameter  $A_1$  (reflecting the nonlinear strength of bending–longitudinal coupling of shafting) will be discussed with the multi-scale method<sup>[23]</sup>. The calculation results are shown in Fig. 7. From the figure, the nonlinear effect of bending–longitudinal coupling can be suppressed by increasing the bearing stiffness of the back stern within a certain range. The nonlinear effect of bending–longitudinal coupling can be enhanced by enlarging the bearing stiffness of the front stern and thrust bearing stiffness within a certain range. The influence of interme-

diate bearing on the bending–longitudinal coupling effect is small. The bending–longitudinal coupling effect can also be enhanced by increasing the propeller mass and reducing the slenderness ratio.

The influence mechanism of shafting parameters on the bending–longitudinal coupling effect of the system is as follows:

1) The first-order bending vibration mode of the propulsion shafting is generally represented as the vibration at the propeller. Therefore, increasing the back–stern bearing stiffness or reducing the propeller mass can effectively reduce the bending vibration of shafting, thereby suppressing the bending–longitudinal coupling effect of the shafting.

2) For the first-order longitudinal vibration of the shafting, since the thrust bearing stiffness is generally much smaller than the tensile or compression stiffness of the shafting itself, the first-order longitudinal

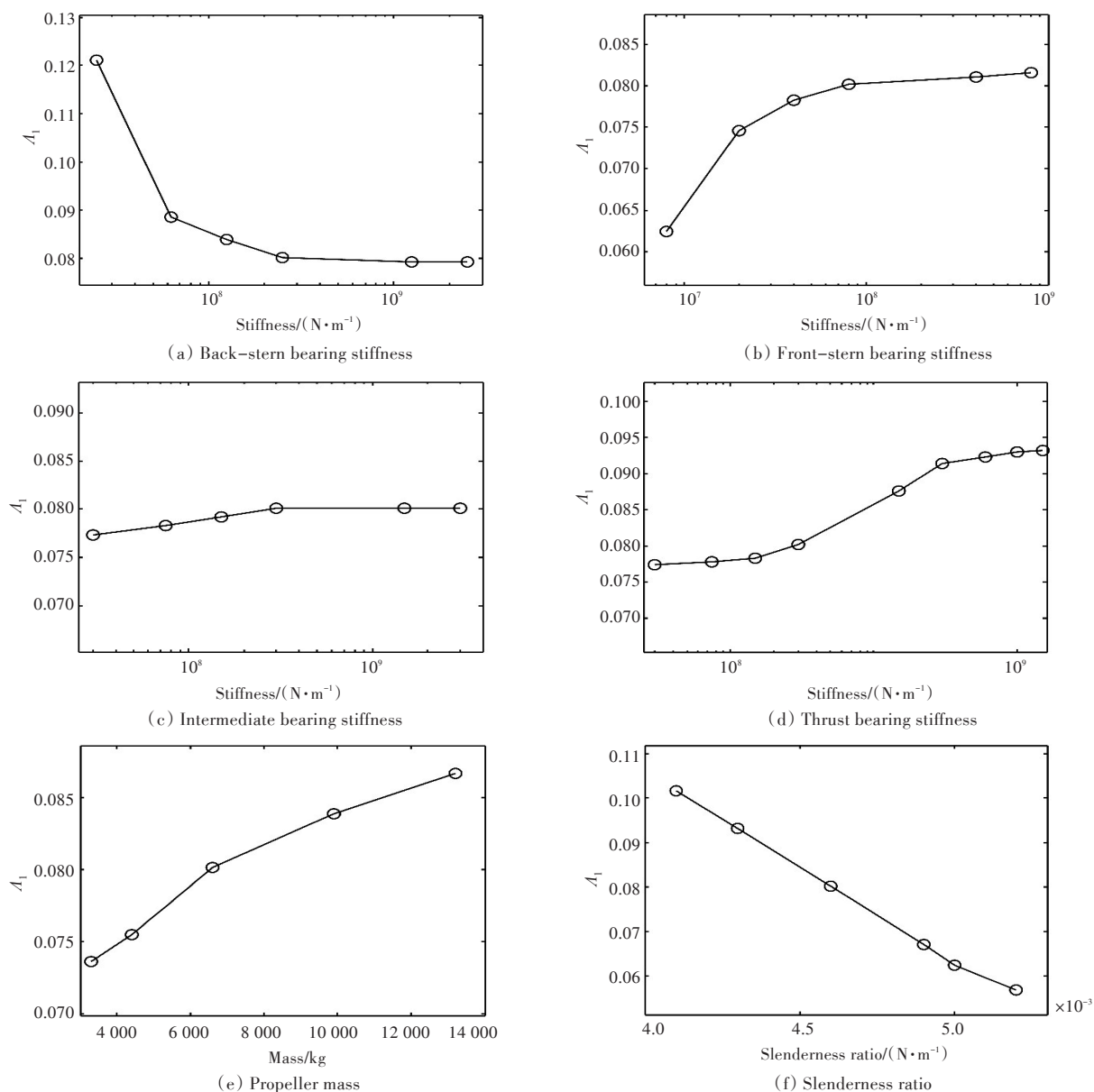


Fig.7 Effect of the shaft parameters on the geometric nonlinear



mode is dominated by the overall translation of shafting. This vibration mode will not cause longitudinal deformation of the shafting, so it will not cause the bending–longitudinal coupling effect of the shafting. However, as the thrust bearing stiffness grows, when its value is equivalent to the tensile or compression stiffness of the shafting itself, the first–order longitudinal vibration of the shafting will no longer be represented as an overall translation but the longitudinal deformation of the shafting itself. At this time, the shafting will produce a significant bending–longitudinal coupling effect. Meanwhile, as the thrust bearing stiffness rises, the bending–longitudinal coupling effect of the shafting becomes stronger and stronger. The influence rule of the front stern bearing on the first–order bending vibration is similar to that on the longitudinal vibration, so it will not be explained in this paper.

3) Since the intermediate bearing is located at the front end of the shafting, its influence on the first–order bending vibration mode of the shafting is very small. Therefore, the influence on the bending–longitudinal coupling effect of the system is also not obvious.

4) The increase in the slenderness ratio of shafting can effectively increase the shafting stiffness, thus reducing the bending and longitudinal deformation of the shafting and finally suppressing the bending–longitudinal coupling effect of the shafting.

## 4 Conclusions

In this paper, the partial differential equation of nonlinear vibration of shafting under bending–longitudinal coupling is established. The solutions to nonlinear equations by FEM and multi–scale method are described, and the influence of bending–longitudinal coupling effect on the nonlinear vibration characteristics of shafting is analyzed. The following conclusions are obtained:

1) Compared with the linear model, the bending–longitudinal coupling effect will increase the natural frequency of the shafting.

2) When the bending–longitudinal coupling effect of shafting occurs, the vibration response of shafting will have complex vibration phenomena such as multi–frequency response, jumping response, and energy migration.

3) The bending–longitudinal coupling effect of shafting can be suppressed by enlarging the back–stern bearing stiffness, which can be enhanced by increasing the front–stern bearing stiffness and

thrust bearing stiffness. However, the influence of intermediate bearing on the bending–longitudinal coupling effect is small.

4) The larger excitation load and the smaller damping ratio can lead to the stronger bending–longitudinal coupling effect of shafting.

## References

- [1] Liu G Y, Lu K, Zou D L Z, et al. Development of a semi–active dynamic vibration absorber for longitudinal vibration of propulsion shaft system based on magnetorheological elastomer [J]. *Smart Materials and Structures*, 2017, 26(7): 075009.
- [2] Zhou L B, Duan Y, Sun Y D, et al. Review of whirling vibration of surface ship propulsion shafting system [J]. *Shipbuilding of China*, 2017, 58(3): 233–244 (in Chinese).
- [3] Li Q C, Yu Q, Liu W. Effect of supporting parameters on marine shaft vibration characteristics [J]. *Ship Science and Technology*, 2016, 38(6): 101–104 (in Chinese).
- [4] Li L Y, Cao Y P, Zhang Z P. Impact of main engine vibration isolation on marine propulsion shafting transverse vibration under lateral rolling [J]. *Journal of Vibration and Shock*, 2016, 35(24): 201–206 (in Chinese).
- [5] Zhang G B, Zhao Y, Li T Y, et al. Propeller excitation of longitudinal vibration characteristics of marine propulsion shafting system [J]. *Shock and Vibration*, 2014, 2014: 413592.
- [6] Zhang J G, Tian J B, He T. Analysis on shafting axial vibration of marine thrust bearing considering pad geometrical parameters [J]. *Chinese Journal of Ship Research*, 2018, 13(Supp 1): 142–146, 164 (in Chinese).
- [7] Hu Z C, He L, Xu W, et al. Optimization design of resonance changer for marine propulsion shafting in longitudinal vibration [J]. *Chinese Journal of Ship Research*, 2019, 14(1): 107–113 (in Chinese).
- [8] Zhang Y Y, Lou J J. Study on longitudinal vibration characteristic and control technology of propulsion shafting [J]. *Journal of Ordnance Equipment Engineering*, 2016, 37(1): 23–26 (in Chinese).
- [9] Polic D, Ehlers S, Aesoy V. Propeller torque load and propeller shaft torque response correlation during ice–propeller interaction [J]. *Journal of Marine Science and Application*, 2017, 16(1): 1–9.
- [10] Tan W Z, Zhang C, Tian Z, et al. Research on the characteristics of torsional vibration of large–scale ship propulsion shafting [J]. *Ship Science and Technology*, 2015, 37(1): 45–49 (in Chinese).

- [11] Hua C L, Cao G H, Rao Z S, et al. Coupled bending and torsional vibration of a rotor system with nonlinear friction[J]. Journal of Mechanical Science and Technology, 2017, 31(6): 2679–2689.
- [12] Hua C L. Study on dynamic characteristics of the rotor–rubber bearing system with rub–impact [D]. Shanghai: Shanghai Jiao Tong University, 2014 (in Chinese).
- [13] Zhang Z G, Zhang Z Y, Chen F, et al. Research on the coupling between torsional and lateral vibrations in propeller–shaft system with friction[J]. Journal of Mechanical Engineering, 2013, 49(6): 74–80 (in Chinese).
- [14] Liu Z F, Hu Y, He Y W, et al. Transient analysis and fatigue life calculation of shaft system based on bend–torsion coupling[J]. Internal Combustion Engines, 2017(4): 38–42 (in Chinese).
- [15] Zhu H H, Zhang X M, Liu Z L, et al. Analysis on the property of ship shafting bending–torsion vibration coupling with bearing lubrication under impulse load[J]. Journal of Ship Mechanics, 2010, 14(1/2): 126–131 (in Chinese).
- [16] Jiang H, Jiang W K. Study of lateral–axial coupling vibration of propeller–shaft system excited by nonlinear friction [J]. Archive of Applied Mechanics, 2016, 86(8): 1537–1550.
- [17] Zou D L, Zhang J B, Ta N, et al. Coupled longitudinal–transverse nonlinear dynamics of a marine propulsion shafting–primary resonance under blade frequency excitation[J]. Journal of Ship Mechanics, 2017, 21(2): 201–210 (in Chinese).
- [18] Yang Z R, Zou D L, Rao Z S, et al. Responses of longitudinal and transversal nonlinear coupling vibration of ship shafting [J]. Journal of Ship Mechanics, 2014, 18(12): 1482–1494.
- [19] Zou D L, Liu L, Rao Z S, et al. Primary resonances of shafts with coupled longitudinal–transverse vibration by finite element and shooting methods[J]. Journal of Vibration Engineering, 2016, 29(1): 87–95 (in Chinese).
- [20] Zou D L, Jiao C X, Ta N, et al. Forced vibrations of a marine propulsion shafting with geometrical nonlinearity (primary and internal resonances)[J]. Mechanism and Machine Theory, 2016, 105: 304–319.
- [21] Zou D L, Xun Z Y, Rao Z S, et al. Dynamic analysis of the coupled longitudinal–transverse shafts under primary and internal resonances[J]. Journal of Vibration Engineering, 2016, 29(3): 511–520 (in Chinese).
- [22] Zou D L, Liu L, Rao Z S, et al. Coupled longitudinal–transverse dynamics of a marine propulsion shafting under primary and internal resonances[J]. Journal of Sound and Vibration, 2016, 372: 299–316.
- [23] Zou D L, Rao Z S, Ta N. Coupled longitudinal–transverse dynamics of a marine propulsion shafting under superharmonic resonances[J]. Journal of Sound and Vibration, 2015, 346: 248–264.

## 船舶推进轴系弯—纵耦合效应的非线性振动特性

徐鹏<sup>1</sup>, 邹冬林<sup>2,3</sup>, 吕芳蕊<sup>2,3</sup>, 塔娜<sup>2,3</sup>, 饶柱石<sup>\*2,3</sup>

1 海军驻大连船舶重工集团有限公司军事代表室, 辽宁 大连 116005

2 上海交通大学 振动、冲击、噪声研究所, 上海 200240

3 上海交通大学 机械系统与振动国家重点实验室, 上海 200240

**摘要:** [目的] 大型船舶的推进轴系一般具有轴系长、跨度大、细长比小等特点, 其弯曲变形与纵向变形之间易存在弹性耦合效应, 从而引起轴系异常振动, 影响轴系的安全稳定运行。为了研究轴系弯—纵耦合的非线性振动特性, [方法] 利用变分原理推导轴系发生弯—纵耦合时的非线性振动方程, 采用有限元法(FEM)、打靶法等数值方法, 以及多尺度法等近似解析方法对非线性方程进行求解, 并对比分析弯—纵耦合效应对轴系非线性振动特性的影响。[结果] 计算结果表明: 弯—纵耦合效应将导致轴系响应中出现多频响应、跳跃现象、能量迁移等复杂的振动现象, 同时将增加轴系弯曲方向和纵向方向的固有频率。[结论] 研究成果可为大型船舶推进轴系的工程设计提供参考。

**关键词:** 推进轴系; 弯—纵耦合; 有限元; 打靶法; 多尺度法